Research Article

Morin Improves LPS-Induced Acute Lung Injury by Regulating DUSP5 to Inhibit Macrophage Pyroptosis and Inflammatory Response

Jing Yu[1]; Yi Cao[2]; Jing Zhao[1]; Tong Su[3]; Qi Xuan Feng[1]; Xueying Gao[4]; Yike Zhang[1]; Zhixiong Ye[1]; Yiming Ma[1]; Kun Tang[1]; Wensen Pan[1]*

[1]Second Department of Respiratory and Critical Care Medicine, The Second Hospital of Hebei Medical University, Shijiazhuang, China.

[2]Department of Geriatric Respiratory Medicine, Hebei Provincial People's Hospital, Shijiazhuang, China.

[3]Medical Department, The Second Hospital of Hebei Medical University, Shijiazhuang, China.

[4]Second Department of Cardiovascular Medicine, The Second Hospital of Hebei Medical University, Shijiazhuang, China.

*Corresponding Author: Wensen Pan

Second Department of Respiratory and Critical Care Medicine, The Second Hospital of Hebei Medical University, Shijiazhuang, China.

Email: 27400010@hebmu.edu.cn

Abstract

Objectives: Acute Lung Injury (ALI) is an acute pneumonia caused by various factors. Current treatments have issues with efficacy and side effects. Morin, a dietary bioflavonoid, exhibits robust anti-inflammatory and antioxidant characteristics. Specifically, it has been observed to exert anti-inflammatory effects on macrophage cells. This study aimed to explore the protective mechanism of Morin on Acute Lung Injury (ALI).

Methods: Broncho Alveolar Lavage (BAL) samples were collected from patients, analyzed by RNA-sequencing and flow cytometry. Additionally, a LPS induced ALI mouse tumor model was constructed. The effects of Morin on the pyroptosis and inflammation of macrophages were evaluated using Immunofluorescence, western blotting, and q-PCR. Macrophage were isolated in vitro to clarify the protective role of Morin. Additional vectors for knockdown of DUSP5 (dual specificity phosphatase 5) gene were established in H9c2 macrophage cell line.

Results: In the Broncho Alveolar Lavage (BAL) samples of patients, the number of macrophages was elevated prior to treatment initiation. Within the pretherapy group, the NLRP3 inflammasome, IL-1β, and IL-18 levels in the BAL of ALI patients exhibited a significant increase. Transcriptomic analysis of BAL samples from patients identified a marked upregulation of DUSP5 in ALI cases, which was subsequently confirmed through q-PCR and western blot analysis. Findings from an ALI mouse model revealed that Morin notably suppressed alveolar injury, reduced the expression of pyroptosis markers NLRP3 and N-GSDMD, enhanced the presence of M2 macrophages, lowered levels of IL-1β and IL-18, and downregulated the DUSP5, ERK1/2, and JNK signaling pathways, thereby mitigating LPS-induced ALI-associated cell apoptosis. In vivo experimentation on macrophages further demonstrated that Morin inhibited macrophage pyroptosis and decreased cellular inflammation. Comparatively, levels of IL-1β and IL-18, the ERK1/2 and JNK signaling pathways, pyroptosis markers NLRP3 and N-GSDMD, as well as macrophage apoptosis, were notably reduced in the siRNA-DUSP5 group when contrasted with the control group. In addition, after adding Morin to cell lines with DUSP5 knocked down, the function of Morin could not be performed. CO-IP experiments found that DUSP5 can interact with the GSDMD. It is speculated that Morin can affect the pyroptosis of macrophages by regulating DUSP5.

Conclusion: Morin improves LPS-induced acute lung injury by regulating DUSP5 to inhibit macrophage pyroptosis and inflammatory response.

Keywords: Acute lung injury; Morin; DUSP5; Macrophage pyroptosis.

Wensen Pan

Introduction

Acute Lung Injury (ALI) is a debilitating clinical syndrome with a consistently high mortality rate, attributed to its intricate pathophysiology and limited treatment options [1,2]. Apoptosis has long been considered one of the potential underlying mechanisms of ALI [3,4]. However, apoptosis is characterized by intact cell membrane structures and a lack of associated inflammatory responses, which do not entirely elucidate the marked inflammatory reaction observed in ALI [5]. In contrast, pyroptosis represents a form of orchestrated cellular demise that is orchestrated by the activation of caspase-1 within the inflammasome, a complex composed of multiple proteins [6]. This process leads to the cleavage and polymerization of Gasdermin D (GSDMD), resulting in the disruption of cellular membrane integrity. The activation of caspases, GSDMD, cellular disintegration, and the substantial release of inflammatory factors are distinctive features that set pyroptosis apart from other programmed cell death pathways [7]. Macrophages, constituting approximately 95% of the lung's leukocytes, assume a pivotal role in ALI, responding to both infectious and non-infectious stimuli by fostering the synthesis and secretion of pro-inflammatory cytokines [8]. Dysregulation of macrophage function contributes to tissue damage and amplifies the inflammatory response in ALI [9].

Recent research has unveiled Morin, a natural compound found in plants belonging to the Moraceae family, as a potential therapeutic target due to its versatile biological and pharmacological properties [10]. Morin, as a dietary bioflavonoid, exhibits robust anti-inflammatory and antioxidant characteristics [10,11]. Specifically, it has been observed to exert anti-inflammatory effects on macrophage cells [11], potentially regulating the inflammatory response in ALI. Nonetheless, the precise role and underlying mechanisms by which Morin modulates macrophages in ALI remain largely unexplored.

To investigate the changes occurring in macrophages and the role played by Morin in ALI, we conducted RNA-Seq analysis and observed an upregulation of the dual-specificity phosphatase 5 (DUSP5) enzyme in macrophages. In a murine model of ALI, we further observed that Morin can modulate the activity of DUSP5, consequently inhibiting macrophage pyroptosis and ameliorating the inflammatory response in ALI. Our study highlights the potential of a therapeutic approach utilizing Morin in the treatment of ALI, with the aim of contributing to the development of effective strategies for managing ALI and its accompanying complications.

Materials and methods

Patients

To investigate inflammation and macrophage alterations in ALI, 24 patients with ALI were enrolled at the Second Hospital of Hebei Medical University between September 2018 and September 2022. The median age of ALI patients was 57.6 years (range, 46–67 years). ALI clinical responses to treatment were determined according to established guidelines.

To explore the effects of on ALI macrophages, we collected Broncho Alveolar Lavage (BAL) samples before and at least 1 weeks after treatment (for pretherapy evaluation) and at least 2 months after treatment (for posttreatment evaluation). Samples were immediately centrifuged and macrophages were harvested for further experiments, including flow cytometry, ELISA, RNA-seq, q-PCR and Western blot. All patients' samples were collected in compliance with ethical requirements, and patients' informed consent had been obtained.

Mice

The acute lung injury mouse model induced by LPS was established using male C57BL/6J mice (8 weeks old, weighing 20–22 g) obtained from Second Department of Respiratory and Critical Care Medicine Animal Care. The animals were housed in specific pathogen-free conditions with a 12-hour light-dark cycle, appropriate temperature, and humidity.

Mice were exposed to LPS in an acrylic chamber. A 0.5 mg/mL solution of LPS (L2880, Sigma-Aldrich, MO, USA) was prepared in saline. The aerosolized LPS was delivered into the acrylic chamber (29 cm × 24 cm × 16 cm) using an air pump and regulated with a manometer to achieve a specific flow rate (1 mL/min) for 30 min. After atomization for 30 min, the interval was 2 h, then atomized for 30 min again, and the experiment endpoint was in 4 h. Mice were randomly divided with eight mice per group.

Cells and reagents

Human interleukin-1β (IL-1β) ELISA Kit: (Lot: HM10206, Beinlai Biotechnology, Hubei, China); Human interleukin-18 (IL-18) ELISA Kit: (Lot: HM10337, Beinle Biotechnology, Hubei, China); Mouse interleukin-1β (IL-1β) ELISA Kit: (Lot: HM20206, Beinlai Biotechnology, Hubei, China); Mouse interleukin-18 (IL-18) ELISA Kit: (Lot: HM21337, Beinle Biotechnology, Hubei, China); TUNEL Cell Apoptosis Detection kit-Cy3 ((Lot: MK1012, Beinle Biotechnology, Hubei, China).

Immunofluorescence

After mice were sacrificed, lung tissues were excised. The lung tissues were fixed in 4% paraformaldehyde at room temperature and then embedded in paraffin. Sections (5 μm) were cut. Histopathological evaluation was observed by two independent investigators blinded to the experimental conditions. For immunohistochemistry, tissue sections were blocked with 10% normal horse serum and incubated overnight at 4°C in a humidified environment with Arg1 mAb (Lot: ab239731, Abcam, Cambridge, MA, UK), iNOS mAb (Lot: ab178945, Abcam, Cambridge, MA, UK), NLRP3 mAb (Lot: ab283819, Abcam, Cambridge, MA, UK) and N-GSDMD antibody (Lot: DF13758, Ambion, Austin, TX, USA). Primary labeling was detected using biotinylated horse anti-rabbit IgG secondary antibody (Lot: ab328919, Abcam, Cambridge, MA, UK). All images were captured using a Leica TCS SPS microscope (LX23, Leica, Wetzlar, Germany).

Hematoxylin and Eosin (HE) staining

Sections affixed to glass slides, placed in a 42°C oven overnight, and baked at 60°C for 1 hour. Deparaffinization and rehydration were performed using a gradient of alcohol. After deparaffinization, the sections were soaked in distilled water, to wash off the alcohol. Hematoxylin staining of cell nuclei was performed by staining with hematoxylin solution for 2 minutes. After differentiation with 1% hydrochloric acid alcohol, eosin

staining was performed for 3 minutes. Dehydration and sealing of the sections were carried out by sequentially placing the sections in 70%, 80%, 95% ethanol solutions, absolute ethanol, a 1:1 mixture of ethanol and xylene, and xylene, followed by air-drying and sealing with neutral gum. Microscopic observation and photography were conducted.

Immunohistochemical staining

The process of deparaffinization of paraffin sections is the same as that of HE staining. Antigen retrieval: Place the sections in citric acid retrieval solution and heat in a microwave on high for 5 minutes. Quickly transfer the repaired tissue sections to preheated distilled water. 3% H_2O_2 is dripped onto the sections, and the reaction is carried out in a dark box to remove endogenous peroxidase. Add 0.1% Triton X-100 for membrane permeabilization. Block with goat serum at room temperature for 1 hour. Incubation with primary antibody: Add NLRP3 primary antibody (Lot: ab283819, Abcam, Cambridge, MA, UK, 1:100), N-GSDMD primary antibody (Lot: DF13758, Ambion, Austin, TX, USA, 1:100) to the sections. Incubation with secondary antibody: Add HRP-labeled goat anti-rabbit IgG secondary antibody (Lot: ab6721, Abcam, Cambridge, MA, UK, 1:200), HRP-labeled goat anti-mouse IgG secondary antibody (Lot: ab209715, Abcam, Cambridge, MA, UK, 1:200) to the sections, and incubate in the dark at room temperature for 60 minutes. Use a microscope for observation and photography. Subsequently, the immunohistochemical staining intensity is quantified.

TUNEL staining

Cells were stained with TUNEL working solution, washed with PBS, and then stained with DAPI to label the cell nuclei. Anti-fade mounting medium was added to fix the cells, which were then air-dried at room temperature and observed under a fluorescence microscope to assess apoptosis. The TUNEL-positive cells were marked by green fluorescence, representing apoptotic cells, while the cell nuclei were marked by blue fluorescence. Six random fields were selected for cell counting, and the ratio of TUNEL-positive cells to total cells was recorded as the TUNEL-positive cell ratio.

Flow cytometry

BAL samples were analyzed using Anti-NLRP3 antibody (Lot: ab263899, Abcam, Cambridge, MA, UK), Goat anti rabbit IgG (Alexa Fluor 488) (Lot: ab150077, Abcam, Cambridge, MA, UK) was used as an indirect labeling reagent for biotinylated antibodies. Dead cells were excluded by DAPI labeling (Lot: 5079, Sigma-Aldrich, St. Louis, MO, USA).

Macrophage bulk RNA-Seq

Total RNA was extracted from isolated human macrophages using a RNeasy Micro Kit (Lot: 14043, QIAGEN, Duesseldorf, Germany). Sequencing libraries were generated using a NEBNext Ultra RNA Library PrepKit for Illumina following the manufacturer's recommendations. After quantification and quality assessment, mRNA was purified with oligo-dT magnetic beads for library preparation. First-strand cDNA was synthesized using a random hexamer primer and M-MuLV Reverse Transcriptase. Second-strand cDNA synthesis was subsequently performed using DNA Polymerase I and RNase H. After the synthesis of both strands and adenylation of the 3' ends of the DNA fragments, the NEBNext Adaptor with a hairpin loop structure was ligated to prepare the samples for hybridization. The library fragments were purified using an AMPure XP system. Next, PCR amplification was performed using Phusion High-Fidelity DNA polymerase, universal PCR primers, and an index (X) primer. The PCR products were purified using the AMPure XP system. The index-coded samples were clustered using a TruSeq Cluster Kit v3-cBot-HS, and library preparations were sequenced on an Illumina NovaSeq platform. Differential expression analysis was performed using the DESeq2 R package. Genes with an adjusted P value of less than 0.05, found by DESeq2, were assigned as differentially expressed.

RNA isolation and qPCR

RNA was extracted from isolated macrophages using a RNeasy Mini Kit (Lot: 241343, QIAGEN, Duesseldorf, Germany) and then reverse transcribed into cDNA with the Reverse Transcription System. qPCR was conducted using SYBR Green PCR Master Mix. The housekeeping gene GAPDH served as a positive quantitative control, and the relative quantitation of raw data was based on the ΔΔCt method. The primers used in this study were as follows: murine Gapdh, F-5'-AAGTTCATCTGCACCACCG-3' and R-5'-TGCTCAGGTAGTGGTTGTCG-3'; DUSP5: F-5'-GTGCCTACTGCACATTCCCT-3' and R-5'-TCCCGAGAACCTACCCTGAG-3'.

Western blotting

Western blotting was performed as described previously [12]. In brief, total proteins were extracted from cells and resuspended in 5×SDS-PAGE loading buffer. The boiled protein samples were then subjected to SDS-PAGE followed by immunoblotting with DUSP5 antibody (Lot: ab200708, Abcam, Cambridge, MA, UK), GAPDH antibody (Lot: ab8227, Abcam, Cambridge, MA, UK), p-ERK1/2 antibody (Lot: ab278538, Abcam, Cambridge, MA, UK), ERK1/2 antibody (Lot: ab184699, Abcam, Cambridge, MA, UK), p-JNK antibody (Lot: ab124956, Abcam, Cambridge, MA, UK), JNK antibody (Lot: ab179461, Abcam, Cambridge, MA, UK) and HRP labeled sheep anti-Rabbit IgG secondary antibody (Lot: ab7090, Abcam, Cambridge, MA, UK).

RNA interference and *In Vitro* transcribed mRNA of DUSP5

Preparation and microinjection of in vitro-transcribed mRNA were performed. In brief, plasmids containing DUSP5–green fluorescent protein were linearized and used as templates for in vitro transcription using the T7 Message Machine kit (Lot:7651, Ambion, Austin, TX, USA). RNAi-negative control HiGC was used as a control siRNA. The sequence was synthesized by GeneChem Co., Ltd. The sense strand is 5'- AGCTTCCCTGGCTAACGGTCTG-GCGCTGGCTGTTGCTGACTGCTTGTTGTCCGCGCTGGATACTGA-3', and the antisense strand is 5'-CAACGGTTAACTTGTCGACTCT-GAACGGTGTGCTGTTGTGGTGCGCTGGGTTTTGTGAG-3'. Synthesized RNA was polyadenylated further using poly(A) polymerase (Lot:3124, American Research Products, Grandville, MI, USA) and dissolved in 150 mM KCl at a final concentration of ~100 ng/µl. Diluted RNA was filtered, heated at 90°C for 1 min and cooled on ice. Macrophage cell line H9c2 were transfected with DUSP5 siRNA or control siRNA mixed with the transfection reagent (Lot:113158, Eppendorf, Hamburg, Germany; final concentration: 100 nM).

Statistics

Flow Cytometry Standard (FCS) files were analyzed using FlowJo software. Data are represented as the mean ± SEM. At least 3 independent replicates were included for all experiments. One-way ANOVA followed by an unpaired, 2-tailed t test was used to test for statistical differences. Multiple-testing correction was performed by the Holm-Bonferroni method. A P

value of less than 0.05 was considered statistically significant. All calculations were performed using SPSS version 20 (IBM) and R version 3.6.1 (R Foundation for Statistical Computing) software programs.

Results

Elevated activation of pyroptotic biomarkers in patients with acute lung injury from clinical study

We aimed to validate the inflammation profile in different groups by analyzing clinical samples. We compared ALI patients before (pretherapy) and after therapy (posttreatment) (Figure 1). BAL were collected in different time points. We found that compared with pretherapy, macrophage decreased dramatically after the treatment, which means macrophage may play a role in ALI (p<0.001). Before treatment, the number of macrophages were 1250×10^6 in average, while after treatment macrophage in BAL were decreased into 813×10^6 in average (p<0.001) (Figure 1B). The aberrant activation of macrophages may contribute to tissue damage and exacerbate the inflammatory response in ALI.

With activation of macrophages, inflammasome formation is also present in ALI. Macrophage pyroptosis, induced by the activation of the specific NLRP3 inflammasome, considered to be a significant contributor to injury and fibrosis [5]. In addition, the levels of proteins associated with pyroptosis, including GSDMD-N, IL-1b, and IL-18 have been reported that are related to the production of NLRP3 inflammasome [13]. Therefore, we next examined NLRP3 inflammasome in BAL from ALI patients before and after therapy and found that the relative fluorescence intensity of NLRP3 was significantly increased in pretherapy group compared with their posttherapy (0.95% vs. 0.21%, respectively; p<0.001, Figure 1C). Notably, pretherapy group had a stronger effect on inflammation progression than posttreatment. As the BAL in pretherapy group contained a high level of IL-1β and IL-18 (p<0.001, Figure 1D and 1E). The imbalance of M1/M2 macrophage polarization is a key factor in the pathogenesis of ALI. M2 macrophages polarization were induced after treatment (p<0.001, Figures 1F and 1G). Further analysis of macrophage, we found that macrophage pyroptosis occurs, characterized by the cleavage of GSDMD, with subsequent activation of caspase-1 and caspase-4 (Figure 1H and 1I). We thus conclude that during ALI macrophages are activated with increased pyroptosis.

RNA-Seq revealed DUSP5 disruption in patients of ALI

To dissect the alterations in patients of ALI, we collected BAL from control and ALI patients, isolated macrophages and analyzed by RNA-Seq. Cluster analysis revealed significant differences between the transcriptome of macrophages between control and ALI patients (Figure 2A). RNA-Seq analysis resulted in the identification of 423 up-regulated genes and 452 down-regulated genes. Heatmap showed that pyroptosis related genes were obviously activated (Figure 2B). GO data also showed that NOD, caspase-1, TNF and other signaling pathways were activated when ALI occurred, which proved the occurrence of pyroptosis (Figure 2D). Notably, DUSP5 (dual specificity phosphatase 5) gene exhibited significant higher expression in ALI patients (Figure 2C). As expected, various genes involved in activation of macrophages (Figure 2C) were upregulated during ALI versus in control. DUSP5 acts as an anti-inflammatory regulator by inhibiting the ERK and NF-κB signaling pathways induced by LPS in macrophages. According to the prediction protein inter-

action analysis of the bioinformatics database, DUSP5 interacts with GSDMD through genes such as MAPK9 and CASP4, which is speculated to be the signaling pathway of DUSP5 participating in cell pyrodeath (Figure 2E). Thus, we detected DUSP5 expression level though q-PCR and western, our results revealed a significant upregulation of DUSP5 mRNA (p<0.001) and protein (p<0.05) in ALI patients (Figures 2F and 2G). These findings suggest that DUSP5 may be involved in macrophage activation and pyroptosis during ALI.

Morin improves LPS-induced acute lung injury in mouse model

Morin, a natural compound found in plants belonging to the Moraceae family, exhibits robust anti-inflammatory and antioxidant characteristics. Specifically, it has been observed to exert anti-inflammatory effects on macrophage cells. Thus, we hypothesized that Morin potentially regulating the inflammatory response in ALI.

To elucidate the role of Morin in ALI, we established a mouse model of ALI. Prior to aerosolized LPS, mice exhibited no significant differences. By performing HE staining, we confirmed the pathological characteristics and successful establishment of the model. In the Control group, the alveolar structure was intact without obvious pathological changes. However, in LPS-stimulated ALI group, alveolar septum thickening, alveolar cavity narrowing, alveolar edema and congestion were observed. In ALI group with Morin treatment, the degree of inflammatory cell infiltration was reduced (Figure 3A).

Apart from that, though lung tissue immunohistochemical staining, there was lower levels of NLRP3 (Figure 3B) and N-GSDMD (Figure 3C) in ALI group with Morin treatment compared with ALI. All these results indicate that Morin has a protective effect on LPS-induced lung injury, and may modulate macrophage pyroptosis and inflammatory response.

To further clarify the role of Morin in ALI, we use markers of classically activated and alternative activated macrophages, iNOS and Arg1, to identify M1/M2 type macrophages. We observed lower iNOS and higher Arg1 after Morin treatment in ALI (Figure 3D), represent Morin promoted the conversion of M1 to M2 macrophages in ALI. Additionally, there was a significant reduction in the level of IL-1β and IL-18 after Morin treatment in lung tissue (p<0.001) (Fig. 3E-F). DUSP5 was decreased after Morin treatment (p<0.01) (Figure 3G and 3H). Furthermore, the levels of apoptosis in each group were confirmed through Tunel staining, revealing a significant increase in apoptosis in ALI, while after Morin treatment apoptotic cells were decreased (Figure 3I), which consistently indicate that Morin improves LPS-induced ALI in cell apoptosis. Meanwhile, ERK1/2 and JNK signaling pathway were activated in ALI, and Morin treatment suppressed these signaling (Figure 3J). These results indicated that Morin improves LPS-induced ALI by regulating DUSP5.

Morin inhibit macrophage pyroptosis and reduce cellular inflammation *In Vitro*

To corroborate the role of Morin in macrophage, we isolated macrophage from wild type mouse, and using LPS stimulate in vitro during cell culture. Meanwhile, we added Morin into cell culture medium, to further clarify the exact role of Morin in macrophage.

We assessed IL-1β and IL-18 levels in macrophage using Elisa. Our results revealed a significant upregulation of IL-1β and IL-18

after LPS stimulation (p<0.001), and downregulation in LPS with Morin group (Figure 4A and 4B). Apart from that, there was lower levels of NLRP3 (Figure 4C) and N-GSDMD (Figure 4D) in macrophage of Morin treatment compared with LPS. This supports the notion that Morin modulate macrophage pyroptosis and inflammatory response.

To further clarify the mechanism of Morin, we found that DUSP5 in macrophage was decreased after Morin treatment (Figure 4E and 4F). Furthermore, Tunel staining revealing a significant increase in macrophage apoptosis in LPS stimulation, while after Morin treatment apoptotic macrophages were decreased (Figure 4G). Meanwhile, ERK1/2 and JNK signaling pathway were activated after LPS stimulation, and Morin treatment suppressed these signaling (Figure 4H). These pathological changes mirror the manifestations of ALI in vivo, and further validating Morin inhibit macrophage pyroptosis and reduce cellular inflammation by regulating DUSP5.

Suppression of DUSP5 exert inhibitory effects on macrophage pyroptosis and attenuate cellular inflammation.

The results in Figure 3G and 4F demonstrate that the expression of DUSP5 in ALI tissues is higher than control, while after Morin treatment DUSP5 in macrophage were decreased. This suggests that DUSP5 may play a promoting role in macrophage during ALI.

To understand the role of DUSP5 in macrophage, we used transfection siRNA of DUSP5 in H9c2 macrophage cell line, and results indicate that expression of IL-1β and IL-18 in siRNA-DUSP5 group is lower than in the siRNA-NC group (Figure 5A and 5B). Meanwhile, ERK1/2 and JNK signaling pathway were downregulated in siRNA-DUSP5 group (Figure 5C), indicating that suppression of DUSP5 attenuate cellular inflammation. As Morin may affect the pyroptosis of macrophage, we tested the expression of NLRP3 and N-GSDMD in siRNA-DUSP5 and siRNA-NC group, and the expression of NLRP3 (Figure 5D) and N-GSD-MD (Figure 5E) in the siRNA-DUSP5 group is lower than in the siRNA-NC group, further confirming that suppression of DUSP5 exert inhibitory effects on macrophage pyroptosis (Figure 5E). Tunel staining assays were conducted to assess the apoptosis of macrophage. The apoptotic macrophage transfected with siR-NA-DUSP5 was lower than that of the control group (Figure 5F).

In addition, in order to verify the molecular function of Morin, we added Morin to cell lines with DUSP5 knocked down, and found that the function of Morin could not be performed after knocking down. We found that there was no significant difference in the expression of IL-1A and IL-18 when DUSP5 was knocked down and morin was added (Figure 5G). In addition, NLRP3, GSDMD and Tunel showed no specific changes in pyroptosis indicators after DUSP5 was knocked down, compared with DUSP5 alone (Figure 5H and 5J). We further analyzed the ERK/JNK signaling pathway and found that the addition of morin after knocking down DUSP5 has no effect on activation of ERK/JNK signaling (Figure 5K). These data all proved that morin could not play a role after blocking DUSP5. To further clarify the mechanism, we conducted CO-IP experiments and found that DUSP5 can interact with the GSDMD of pyroptosis related signals (Figure 5L). It is speculated that Morin can affect the pyroptosis of macrophages by regulating DUSP5. All these data indicated that inhibition of DUSP5 reduces the pyroptosis of macrophage and attenuate cellular inflammation.
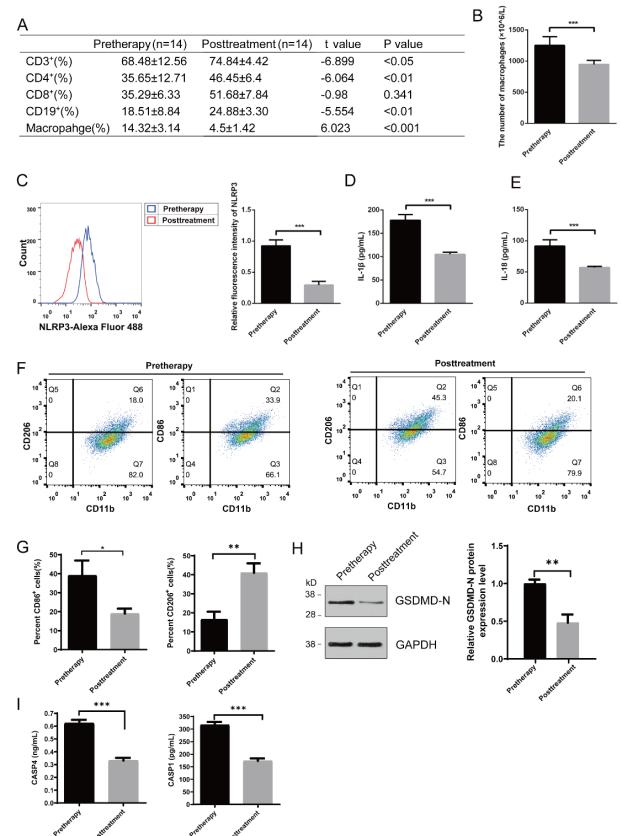

Figure 1: Elevated Activation of Pyroptotic Biomarkers in Patients with Acute Lung Injury from Clinical Study. **(A)** Comparison of CD3⁺T, CD4⁺T, CD8⁺T cells, CD19⁺B cell and macrophage level between pretherapy and posttreatment in ALI patients (x+s). **(B)** Changes in the number of macrophages in the alveolar lavage fluid of each group. **(C)** Flow cytometry analysis of the macrophage pyroptosis marker protein NLRP3 in BAL (bronchoalveolar lavage) of each group. **(D)** ELISA for IL-1β. **(E)** ELISA for IL-18. **(F)** Flow analysis. ***p<0.001. Pretherapy and posttreatment patients with ALI: n=14; n=14 independent replicates.
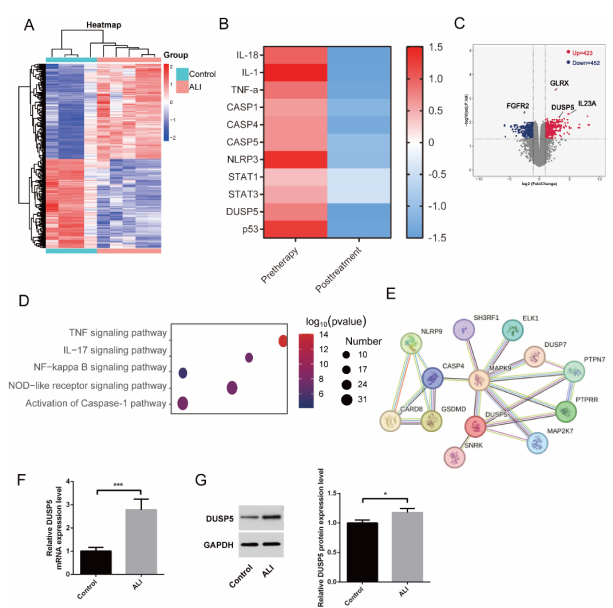

Figure 2: RNA-Seq revealed DUSP5 disruption in patients of ALI. **(A)** Heatmap of differentially expressed genes. **(B)** Heatmap of selected pyroptosis genes. **(C)** Differentially expressed genes. **(D)** GO term of differentially expressed genes. **(E)** Protein interaction network between DUSP5 and GSDMD. **(F)** q-PCR validation of differential DUSP5. **(G)** WB validation of differential DUSP5. *p<0.05, ***p<0.001. Pretherapy and posttreatment patients with ALI: n=14; n=14 independent replicates.

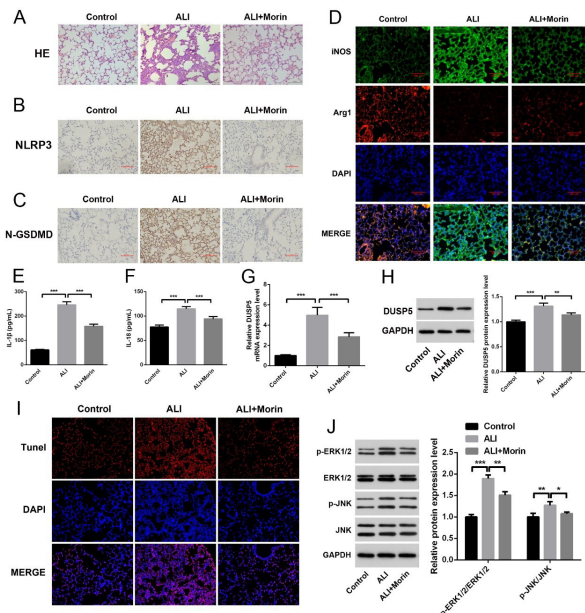**Figure 3:** Morin improves LPS-induced acute lung injury in mouse model. **(A)** HE staining of pathological structure in each group. **(B)** Immunohistochemistry of pyroptosis marker proteins NLRP3. **(C)** Immunohistochemistry of pyroptosis marker proteins N-GSDMD. **(D)** Immunofluorescence staining in macrophage polarization marked by of iNOS and Arg1. **(E)** Elisa of IL-1β in lung tissues. **(F)** Elisa of IL-18 in lung tissues. **(G)** qPCR of differential DUSP5 in lung tissues. **(H)** WB of differential DUSP5 in lung tissues. **(I)** Tunel staining in the lung tissues. **(J)** WB analysis of the regulation of signaling pathway proteins P-ERK1/2, ERK1/2, P-JNK, JNK. *p<0.05, **p<0.01, ***p<0.001. each group n=6 independent replicates.

Figure 4: Morin inhibit macrophage pyroptosis and reduce cellular inflammation in vitro. **(A)** Elisa of IL-1β in each group of cells. **(B)** Elisa of IL-18 in each group of cells. **(C)** Immunohistochemistry of pyroptosis marker proteins NLRP3. **(D)** Immunohistochemistry of pyroptosis marker proteins N-GSDMD. **(E)** qPCR of differential DUSP5 in macrophage. **(F)** WB of differential DUSP5 in macrophage. **(G)** Tunel staining of macrophage. **(H)** WB analysis of the regulation of signaling pathway proteins P-ERK1/2, ERK1/2, P-JNK, JNK. *p<0.05, **p<0.01, ***p<0.001. each group n=6 independent replicates.
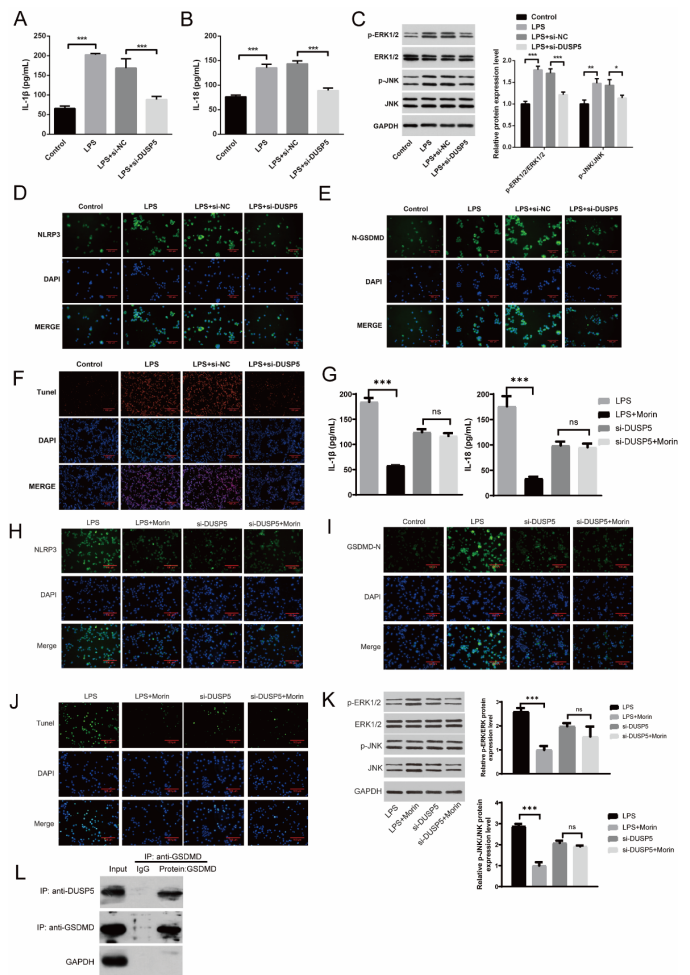

Figure 5: Suppression of DUSP5 exert inhibitory effects on macrophage pyroptosis and attenuate cellular inflammation. **(A)** Elisa of IL-1β in each group of cells. **(B)** Elisa of IL-18 in each group of cells. **(C)** WB analysis of the regulation of signaling pathway proteins P-ERK1/2, ERK1/2, P-JNK, JNK. **(D)** Immunohistochemistry of pyroptosis marker proteins NLRP3. **(E)** Immunohistochemistry of pyroptosis marker proteins N-GSDMD. **(F)** Tunel staining of macrophage. **(G)** Elisa of IL-1β and IL-18 in each group of cells. **(H)** Immunohistochemistry of pyroptosis marker proteins NLRP3. **(I)** Immunohistochemistry of pyroptosis marker proteins N-GSDMD. **(J)** Immunohistochemistry of Tunel. **(K)** WB analysis of the regulation of signaling pathway proteins P-ERK1/2, ERK1/2, P-JNK, JNK. **(L)** CO-IP of DUSP5 and GSDMD. *p<0.05, **p<0.01, ***p<0.001. each group n=6 independent replicates.

Discussion

Acute Lung Injury (ALI) is a severe pneumonia condition caused by various factors, and its current treatment options have limited efficacy and significant side effects [14]. Therefore, there is a pressing need to explore new and effective drugs for ALI treatment. Morin, a dietary bioflavonoid, has shown promising anti-inflammatory and antioxidant properties [15]. Specifically, it has been observed to have anti-inflammatory effects on macrophage cells [16]. This study aimed to investigate the protective mechanism of Morin in ALI.

Analysis of BAL samples from ALI patients revealed higher numbers of macrophages prior to treatment. In the pretherapy group, NLRP3 inflammasome, IL-1β, and IL-18 levels in BAL were significantly increased. RNA-sequencing of BAL samples identified a significant upregulation of the DUSP5 gene in ALI patients, which was further confirmed by q-PCR and Western blot analysis. In the ALI mouse model, Morin treatment significantly reduced alveolar injury, decreased pyroptosis mark-
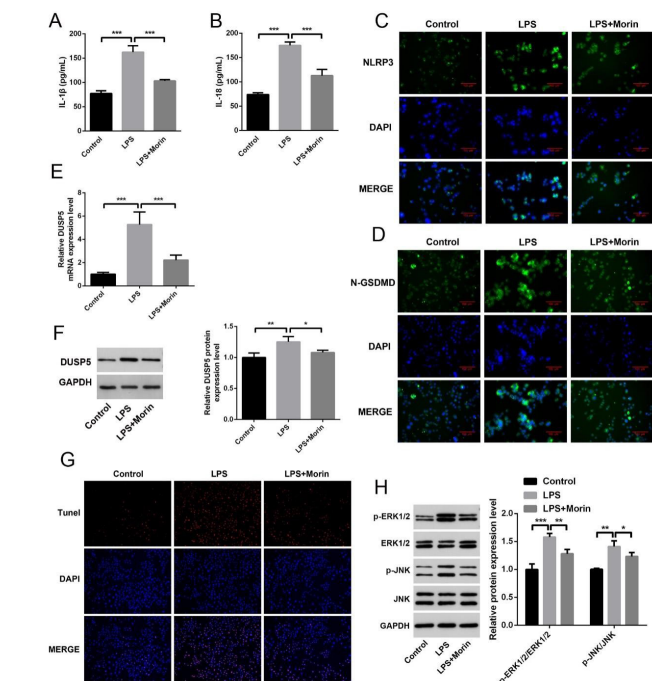
ers NLRP3 and N-GSDMD, enhanced the presence of M2 macrophages, reduced IL-1β and IL-18 levels, and downregulated the DUSP5, ERK1/2, and JNK signaling pathways. Morin treatment also attenuated LPS-induced ALI cell apoptosis. In an in vitro experiment with macrophages, Morin was found to inhibit macrophage pyroptosis and reduce cellular inflammation, as indicated by lower levels of IL-1β and IL-18, decreased activation of the ERK1/2 and JNK signaling pathways, reduced expression of pyroptosis markers (NLRP3 and N-GSDMD), and decreased macrophage apoptosis in the siRNA-DUSP5 group compared to the control group.

One limitation of the study is the relatively limited methods used for detecting pyroptosis. Pyroptosis is a complex form of cell death with distinct molecular characteristics, and relying on a single detection method may not capture the full complexity of this process [17]. To gain a more comprehensive understanding of pyroptosis and its modulation by Morin, future research should consider employing a wide range of techniques, such as live-cell imaging, multiplex assays, or functional assays targeting specific molecular markers associated with pyroptosis. Expanding the repertoire of detection methods can provide a more detailed and nuanced insight into the role of pyroptosis in acute lung injury and the potential therapeutic effects of Morin. Furthermore, while the research emphasized Morin's role in inhibiting macrophage pyroptosis through DUSP5 regulation, a more detailed mechanistic understanding is needed. Future studies should explore additional detection techniques and delve deeper into the molecular pathways involved to enhance comprehension of Morin's therapeutic efficacy in Acute Lung Injury (ALI).

Conclusion

Morin exerts a protective effect against LPS-induced ALI by regulating the DUSP5 gene to inhibit macrophage pyroptosis and inflammatory response. This study sheds light on the potential use of Morin as a therapeutic agent for ALI treatment and provides valuable insights into the underlying protective mechanism. Further research is warranted to explore the clinical applications of Morin in ALI management.

Declarations

Conflict of interest: All authors have completed the ICMJE uniform disclosure form. The authors have no conflicts of interest to declare.

Ethics approval and consent to participate: All human studies were approved by the IRBs of the Second Hospital of Hebei Medical University, Shijiazhuang, China. Each patient (or a legal guardian) provided signed informed consent for therapy, and the collection of prospective data was conducted in accordance with the Declaration of Helsinki. Animal experiments were approved by the IACUC of Second Department of Respiratory and Critical Care Medicine.

Author contributions: Jing Yu performed the experiments, analyzed the data, and wrote the manuscript. Yi Cao, Jing Zhao, Tong Su, QiXuan Feng, Xueying Gao helped with the experiments. Yike Zhang, Zhixiong Ye, Yiming Ma, Kun Tang helped with RNA Seq analysis. Wensen Pan proposed and designed the study, interpreted the results, wrote the manuscript, and oversaw the project.

Availability of data and materials: All data generated or analyzed during this study are included in this article. Further inquiries can be directed to the corresponding author.

References

1. Sun F, Zhang L, Shen L, Wang C. Network Pharmacology Analysis of the Therapeutic Potential of Colchicine in Acute Lung Injury. Int J Clin Pract. 2024; 2024: 9940182.

2. Long ME, RK Mallampalli, JC Horowitz. Pathogenesis of pneumonia and acute lung injury. Clin Sci (Lond). 2022; 136: 747-769.

3. Ju M, Liu B, He H, Gu Z, Liu Y, Su Y, et al. MicroRNA-27a alleviates LPS-induced acute lung injury in mice via inhibiting inflammation and apoptosis through modulating TLR4/MyD88/NF-κB pathway. Cell Cycle. 2018; 17: 2001-2018.

4. Wang JF, Wang YP, Xie J, Zhao ZZ, Gupta S, Guo Y, et al. Upregulated PD-L1 delays human neutrophil apoptosis and promotes lung injury in an experimental mouse model of sepsis. Blood. 2021; 138: 806-810.

5. Jiao Y, Zhang T, Zhang C, Ji H, Tong X, Xia R, et al. Exosomal miR-30d-5p of neutrophils induces M1 macrophage polarization and primes macrophage pyroptosis in sepsis-related acute lung injury. Crit Care. 2021; 25: 356.

6. Liu P, Yang S, Shao X, Li C, Wang Z, Dai H, et al. Mesenchymal Stem Cells-Derived Exosomes Alleviate Acute Lung Injury by Inhibiting Alveolar Macrophage Pyroptosis. Stem Cells Transl Med. 2024.

7. Rao Z, Zhu Y, Yang P, Chen Z, Xia Y, Qiao C, et al. Pyroptosis in inflammatory diseases and cancer. Theranostics. 2022; 12: 4310-4329.

8. Huang X, Xiu H, Zhang S, Zhang G. The Role of Macrophages in the Pathogenesis of ALI/ARDS. Mediators Inflamm. 2018; 2018: 1264913.

9. Chen X, et al. Macrophage polarization and its role in the pathogenesis of acute lung injury/acute respiratory distress syndrome. Inflamm Res. 2020; 69: 883-895.

10. Rajput SA, XQ Wang, HC Yan. Morin hydrate: A comprehensive review on novel natural dietary bioactive compound with versatile biological and pharmacological potential. Biomed Pharmacother. 2021; 138: 111511.

11. Caselli A, et al. Morin: A Promising Natural Drug. Curr Med Chem. 2016; 23: 774-91.

12. Mishra M, S Tiwari, AV Gomes. Protein purification and analysis: next generation Western blotting techniques. Expert Rev Proteomics. 2017; 14: 1037-1053.

13. Ran Y, et al. Curcumin Ameliorates White Matter Injury after Ischemic Stroke by Inhibiting Microglia/Macrophage Pyroptosis through NF-κB Suppression and NLRP3 Inflammasome Inhibition. Oxid Med Cell Longev. 2021; 2021: 1552127.

14. Zhang J, et al. YAP1 alleviates sepsis-induced acute lung injury via inhibiting ferritinophagy-mediated ferroptosis. Front Immunol. 2022; 13: 884362.

15. Jiang Y, et al. Morin protects chicks with T-2 toxin poisoning by decreasing heterophil extracellular traps, oxidative stress and inflammatory response. Br Poult Sci. 2023; 64: 614-624.

16. Shi Y, et al. Morin attenuates osteoclast formation and function by suppressing the NF-κB, MAPK and calcium signalling pathways. Phytother Res. 2021; 35: 5694-5707.

17. Li S, et al. NLRP3/caspase-1/GSDMD-mediated pyroptosis exerts a crucial role in astrocyte pathological injury in mouse model of depression. JCI Insight. 2021; 6.